Feasibility of Magnetic Signature-based Detection of Low and High Impedance Faults in Low-voltage Distribution Networks

Anwarul Islam Sifat*†, Fiona Stevens McFadden‡†, Arif Ahmed†, Ramesh Rayudu†, Arvid Hunze‡†
†School of Engineering & Computer Science, Victoria University of Wellington, Wellington, New Zealand
‡Robinson Research Institute, Victoria University of Wellington, Gracefield, Lower Hutt, New Zealand
*Email: anwarul.sifat@vuw.ac.nz

***Abstract*—This article investigates the feasibility of using non-contact magnetic sensor measurements as the basis for the detection of low and high impedance faults in 0.44 kV distribution networks. It is compared with fault detection using current measurement. A harmonic source free power system was simulated in DIgSilent, in which single line to ground faults was staged. Magnetic field intensity was calculated from simulated phase currents and then the potential detection of faults using total harmonic distortion (THD) and Discrete Wavelet Transform (DWT) was assessed. The use of magnetic sensor measurements as the basis for the detection of low and high impedance faults in 0.44 kV distribution networks was shown to be feasible. As with current-based measurements, wavelet analysis was found to be a better method for HIF faults. However, detection schemes proposed for current-based measurements will need to be modified to suit magnetic field measurements as the shape of the magnetic field waveform differs from the current waveform.**

***Index Terms*—Magnetic Sensor, High Impedance Fault, Wavelets, Total Harmonic Distortion, Distribution Network, Discrete Wavelet Transform**

I. Introduction

The detection of faults and the protection of the power system from their impact is one of the important areas of power system study. In todays highly interconnected power systems improper functioning of protection devices and other automatic systems have the potential to jeopardize the entire system integrity [1], for example, via cascade failure [2].

Broadly, faults are classified as low impedance faults (LIF) and high impedance faults (HIF). LIF has a low impedance and thus higher fault current magnitude while HIF has high impedance and thus lower current magnitudes [3].

Due to their high fault current magnitude, LIFs are easily detectable by conventional protection devices such as distance or over-current relays [4], [5], the detection of HIFs, however, is a more challenging task and conventional fault protection devices fail to detect them. HIF faults usually occur when trees come into contact with the conductor. The most influential factors governing the impedance of the fault are moistness of the surface where the fault takes place and the properties of material the surface is made of [6]. HIFs can happen in both bare and flawed insulated conductors. However, faults on exposed conductors could jeopardize human safety as it ignites flammable arcing, which has extreme legal repercussions [7].

The detection of faults is an ongoing problem that draws significant attention from power system researchers [8]–[10].

Researchers have investigated HIF faults and their detection via both physical and computer simulations. The most well-known model to study HIF via computer simulation is the two diode model [11], [12]. Its simplicity and adjustable voltage and current levels lead to its popularity. This model utilizes two diodes connected in parallel with random resistances and random voltage sources in series with each diode. This model injects arcing current into the medium voltage (15 kV) class distribution conductor being studied. In another study [13], modeling and experimental verification of HIF was performed in medium voltage level (20 kV). The authors simulated the fault behavior using ATP/ EMTP program [14] in which the arc model was realized using a universal arc representation [13]. The focus was on the detection of HIF in a power system network by using the Discrete Wavelet Transform (DWT). A very low magnitude (mA level) HIF current has found which varies with fault location. A wavelet based approach to identify HIF at the high voltage level (220 kV) was also proposed by Tai et al. [15], via detection of the distorted phase of the zero sequence current.

Researchers also have conducted experimental studies of faults in real networks with investigation of suitable HIF detection techniques. Based on their experiments in [16], Gadheri et al. proposed a time-frequency domain algorithm for detecting the HIF faults. An HIF fault was staged at the medium voltage level for different fault materials (e.g. tree, concrete, grass, etc.), the HIF phenomena recorded and detection performed. In [17], the HIF fault was initiated at the medium voltage (20 kV) distribution conductor to collect fault data. Wavelet and statistical pattern recognition was used to detect the HIF. These experiments performed single line to ground faults to obtain the transient data of the HIF.

All previous studies of HIF fault detection have been based on current and/or voltage measurements, however, magnetic fields, are an alternate measurement domain for fault detection, as magnetic fields are generated around current carrying conductors [18].

Magnetic sensors are an attractive basis for fault detection.

978-1-5386-4950-3/17/$31.00 2017 IEEE

They can be implemented as non-contact sensors. These sensors are immune to the biasing factors such fault, ground resistance, and non-homogeneity of line configuration which significantly influence conventional impedance based measurement. Magnetic sensors low cost, small size, and wide operating frequency also make them an attractive measurement technique to use [19].

Magnetic sensor based detection of HIF faults has not specifically been investigated, although they have been investigated for other applications. The application of the Giant Magneto Resistive (GMR) sensor as a current sensor was discussed by Yong et al. [20]. They proposed the addition of a thermal compensator to maintain linearity for high frequency (10 kHz) measurements. This modified GMR sensor showed superior performance for transient-state current measurement compared to other sensors (flux-gate, Shunt, CT, Hall). In [21], Qi Hang et al. investigated a non-contact novel type of sensitive magneto resistive (MR) magnetic sensor to measure currents in high-voltage (500 kV) transmission lines. A numerical simulation was performed using the magnetic field data from sensor and an algorithm proposed to detect the type of fault and its location.

In addition to the detection of HIF faults based on magnetic field measurement being a current research gap, there has been no investigation into the detection of HIF or LIF in the low voltage (0.44 kV) distribution network. Detection of faults in this part of the network is of interest being more extensive, possibly more vulnerable to contact with objects (e.g. trees), that could results in HIF. Now, the question is whether they can give reliable and accurate magnetic measurements for the detection of faults in low voltage networks. However, at this voltage level lower current magnitudes are expected, which presents a more challenging measurement problem for magnetic field based detection of faults.

This paper therefore investigates the feasibility of detecting faults in low-voltage overhead distribution networks using magnetic sensors. This has been carried out via simulation of both low and high impedance faults at various fault locations relative to a single magnetic sensor in a 0.44 kV distribution network. Only a single line to ground fault type has been examined. The resulting magnetic field waveforms have been calculated from the simulated phase currents. Two analysis techniques were then used to evaluate the potential detection of faults from the magnetic fields: i) Total harmonic distortion (THD), a frequency domain analysis and ii) Wavelet analysis. Frequency-domain based fault detection schemes have numerous traditional applications, whereas the wavelet analysis is of current interest in the literature for the detection of faults. About 40% of all the HIF detection techniques have been wavelet based [8].

II. Magnetic Sensor Measurement Principle

The magnetic field of current in the vicinity of a current carrying conductor can be derived by using Maxwell's equations. However,the configuration of overhead lines needs to be taken into account, which can be specific to individual countries. So,

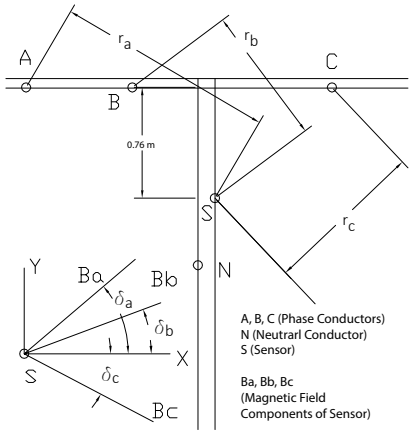

Fig. 1. Tower Configuration and Placement of Sensor

the general equation of the resultant magnetic field detected by a sensor placed on a pole with the configuration as shown in Fig. 1 is given by [22]:

$$\vec{B} = \hat{i_x}[B_a \times cos(\delta_a) + B_b \times cos(\delta_b) + B_c \times cos(\delta_c)]$$

$$+\hat{i_y}[B_a \times sin(\delta_a) + B_b \times sin(\delta_b) - B_c \times sin(\delta_c)] + 0.\hat{i_z} \quad (1)$$

where,

$$B_a = \frac{\mu_0 i_A}{2\pi r_a}, B_b = \frac{\mu_0 i_B}{2\pi r_b}, B_c = \frac{\mu_0 i_C}{2\pi r_c} \quad (2)$$

Here, μ_0 = Magnetic constant; r_a, r_b and r_c are displacements of the conductors from the sensor; i_A, i_B, i_C are the phase currents; δ_a, δ_b, δ_c, are the angle as shown in Fig. 1.

In the above equations, the z-axis component is zero as it is assumed that the z-axis is aligned in the direction of the current flowing in the conductor. It can be observed from the equations that the resultant magnetic field detected by the sensor is dependent on the individual phase current magnitudes and the sensors position relative to the conductors.

III. Overview of Total Harmonic Distortion & Discrete Wavelet Transform

The potential detection of faults from the magnetic field measurement were assessed using: 1) Total harmonic distortion (THD) and 2) Discrete Wavelet Transform (DWT).

Total harmonic distortion (THD), a frequency-domain technique, is the proportional summation of the power of all harmonic components with respect to the power of fundamental frequency. In that regard, it expresses the harmonic attributes of a signal. In power systems this technique has been used to determine distortion of the voltage and current waveforms. We have used it here to characterize and identify the presence of higher frequency components in the waveforms.

Wavelet analysis is a well-developed time-scale domain analysis tool [23]. In power lines, voltages and currents vary simultaneously during faults because fault impedance causes voltage sag in the lines and introduces a inrush transient in the current magnitude. Such transients contain more fault information than the steady-state situation. Wavelet analysis catches both the frequency information and the instant (location) in

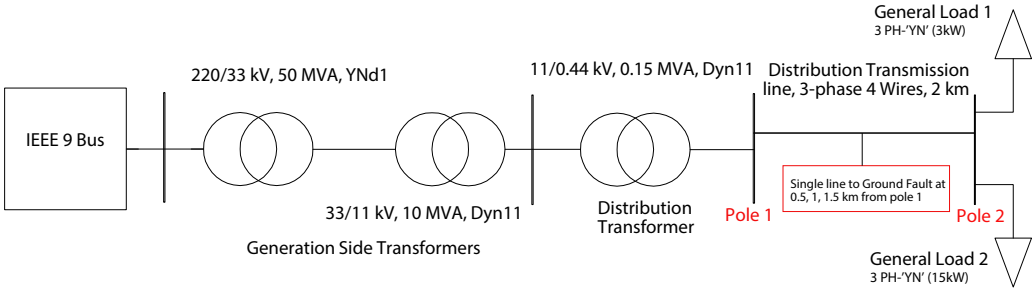

Fig. 2. Schematic Diagram of Network Simulation

time where these frequency components occur. Wavelets are a family of functions, generated from one single function, called the mother wavelet, by means of scaling and translating operations [24]. The Discrete Wavelet Transform (DWT) is the digital version of the Wavelet transform. It gives a number of coefficients based on the integer value of the discretization step in scale and translation. It is of the form:

$$DWT(s,l) = 2^{-s/2} \sum_n X(n) k(2^{-s} n - l) \tag{3}$$

where, s and l are discretization step and translation respectively, determined by $p = 2^s$ and $q = l2^s$. DWT is implemented using a multistage filter with down sampling of the low-pass filter output [25]. The DWT function from the Wavelet toolbox [26] incorporated in the MATLAB program was used in this study, with Daubechies order 4 wavelet as the mother function. The Daubechies wavelet family has been found to be appropriate compare to other wavelet family to localize faults, with Daub4 (db4) a good choice for short and fast anomalous signals [27].

IV. Case Study

For the case study, simulations were performed in DIgSilent Power Factory, a well-known power system simulation software [28]. The IEEE 9 bus network [29] was considered and extended from bus 5 by building a 4 node step-down 0.44 kV distribution system as shown in Fig. 2. The effect of nonlinear loads, capacitor bank switching, harmonic sources and arcing phenomena of HIF current have not been considered in the simulations. The arrangement of the overhead lines consists of 3-phases with one neutral conductor. The line parameters for the simulation were determined from data-sheets and are given in Table I. Considering the conductors in Table I and the pole configuration from [35] as shown in Fig. 1, the sequence impedance matrix is calculated by a modified Carsons equation which is given in Equation 4.

$$[z_{012}] = \begin{bmatrix} 0.75 + j1.66 & 0.02 + j0.01 & -0.03 + j0.01 \\ -0.03 + j0.01 & 0.31 + j0.52 & -0.06 - j0.01 \\ 0.02 + j0.01 & 0.06 - j0.01 & 0.31 + j0.52 \end{bmatrix} \tag{4}$$

As shown in Fig. 2, two poles were simulated (Pole 1 & 2) with the 0.44 kV distribution lines in between. The pole configuration is shown in Fig. 1 according to the data from [30].

TABLE I
Overhead Conductors Standard Manufacture Data [30].

Name	AC Resistance @75 $^\circ C$	*GMR (meter)	Stranding
4/0 ACSR	0.5920	0.00024	6/1
3364000 ACSR	0.306	0.0074	26/7

*GMR = Geometric Mean Radius

Faults were staged in the 0.44 kV overhead line between Pole 1 and 2 (Fig. 2). The fault was initiated at 0.1s and cleared after 60ms. Only a single line to ground fault on phase 'A' was simulated. Various fault resistances and locations were simulated, as detailed in Table II. These resistance values were selected after consideration of literature values for high impedance faults in medium voltage networks and above [17], [31], [32]. No actual data exists for HIF at the low voltage level as no experimental or simulation studies have been performed. For LIF, the resistances were determined based on the definition of an LIF being when the fault current exceeds maximum load current [3], and the choice of values verified by the simulation results (Fig. 3a).

TABLE II
Fault Resistances and Locations Simulated

Fault Impedance	LIF: 1, 5, 10 Ω HIF: 70, 80, 90 Ω
Fault Distance from Magnetic Sensor	0.5, 1, 1.5 km

A 3-axis magnetic sensor was assumed to be placed on Pole 1, at a distance of 0.76 meter below the head of the pole (Fig. 1). Fault current current data was therefore obtained from the simulations at the Pole 1 location. Using equations 1 & 2, the resultant magnetic field, $\vec{B}$, as measured by the magnetic sensor, was calculated from the current data.

V. Results & Discussion

The current waveforms of one of the simulated LIF and HIF are shown in Fig. 3, along with the magnetic field waveform calculated according to the method detailed in Section 3. As expected, for the LIF the current magnitude of phase

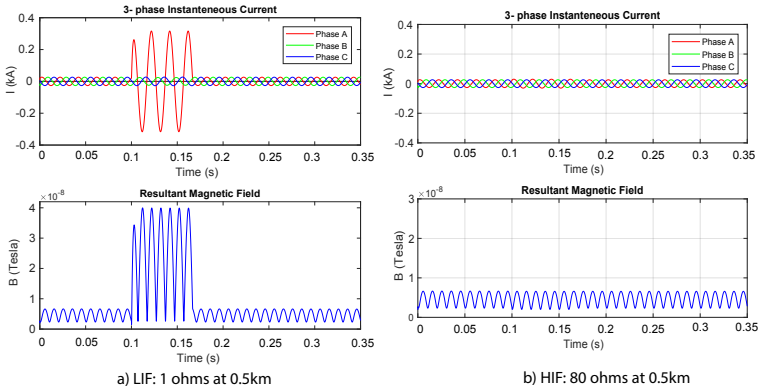

Fig. 3. 3-phase Instantaneous current and resultant magnetic fields (fault occurs from 0.1s to 0.16s)

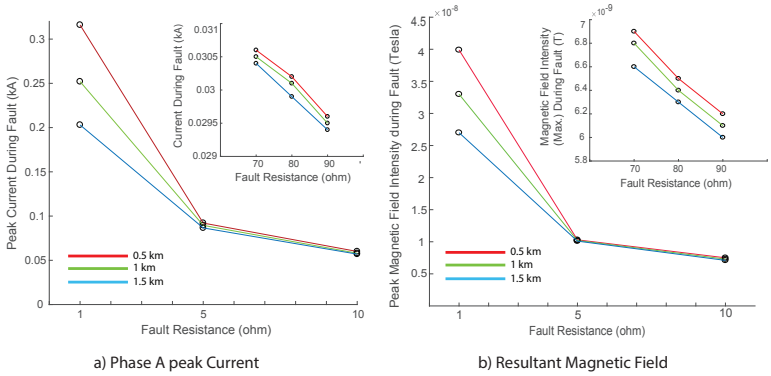

Fig. 4. Peak current in phase A and peak magnetic field during the faults as a function of fault resistance and distance

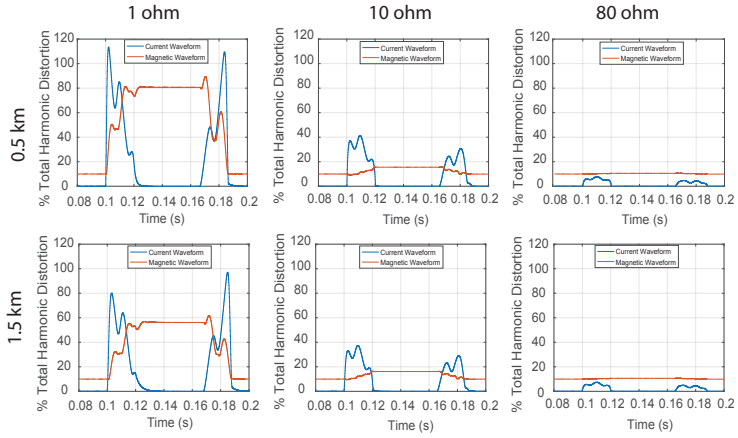

Fig. 5. %THD of phase A current and resultant magnetic field

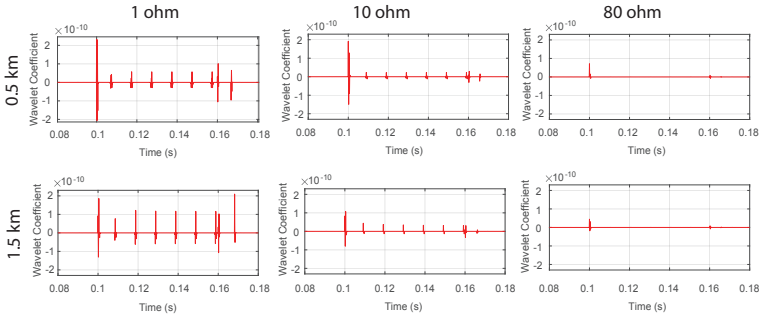

Fig. 6. DWT of phase A current (Daubechies order 4)

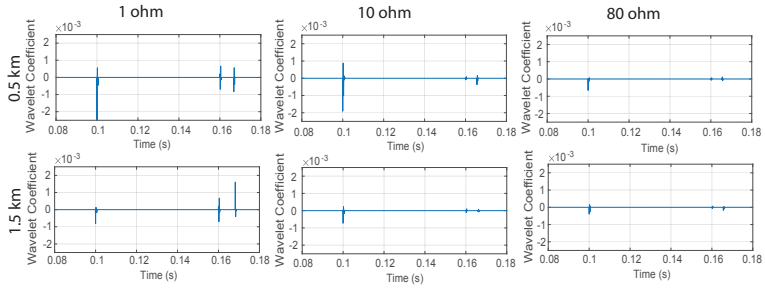

Fig. 7. DWT of magnetic field (Daubechies order 4)

A increases significantly (No fault phase currents 26 amps peak to peak) during the fault while for HIF, only a very small increase is observed. The asymmetry observed in the LIF current waveform is due to negative decaying of the dc component, set by the R/X ratio at the point of the fault. The occurrence of the positive or negative decaying depends on the proximity of a fault to a motor or generator [33], with a constant ac decay if the generator is far from the supply grid [34]. As with the current waveforms, the fault can be readily observed in the magnetic field measurements, with the LIF producing the highest change in magnetic field during the fault. Another interesting feature to note is that during the fault, the magnetic field waveform is no longer sinusoidal, due to the magnitude calculation of $\vec{B}$ components (Equation 1). Fig. 4 summarizes the peak current and resultant magnetic field across all simulated cases. The peak fault current in phase A and resultant magnetic field decreases with increasing resistance (Fig. 4a & b) and to a small extent with increasing fault distance. This is expected due to the relative impedance of the circuit from the transformer to the point of fault.

A. Harmonic Content Analysis

Fig. 5 presents the calculated %THD of the phase A current and of the resultant magnetic field for a subset of the cases simulated. The other cases show similar effects and the results changed in a smooth manner between the different cases so are not presented. The %THD of both the phase 'A' current and the magnetic field is seen to change when the fault is initiated and then subsequently when it is cleared, indicating that frequency-domain based detection of faults from magnetic measurements will perform as well for magnetic field measurements as they do for current measurements. Frequency domain detection schemes would need tailored to the magnetic domain however, as unlike the %THD for the phase current, the %THD of the resultant magnetic field rises more slowly and exhibits a steady value during the fault because the waveform is non-sinusoidal. For both magnetic field and current, the change in %THD for low impedance faults is significantly greater than for high impedance faults, indicating that THD would probably only be useful for the detection of LIF. The results show that the fault current, magnetic field and %THD are only affected marginally by fault distance.

B. Discrete Wavelet Transform

The DWT for Daubechies order 4 for the phase A current and resultant magnetic field are presented in Fig. 6 and 7 respectively. The transients associated with the initiation and clearing of the fault is observed in the DWT of both the phase A current and magnetic signature. As with the THD, due to the non-sinusoidal nature of the magnetic field during the fault, non-zero values occur in the DWT during the fault, hence detection schemes based on DWT would need tailored to the magnetic domain. The DWT coefficients are affected only to a small extent by fault distance. They more significantly decrease with fault resistance, but even for HIF the sharp changes with fault initiation and clearing are still observed.

VI. Conclusion

Our study demonstrates that magnetic sensor based analysis has the potential to be used for fault detection in low-voltage (0.44 kV) distribution networks. As with current measurements, frequency-domain (e.g. %THD) and time-scale domain (e.g. wavelet analysis) of magnetic sensor measurements exhibit the potential to be used to extract the features of the faults. However, due to the different shape of the resultant magnetic field waveform, fault detection schemes developed for current measurements may need to be modified to suit. In future work, more detailed simulations will be performed, for example with the inclusion of harmonic sources and HIF arcing model. Other types of feature extraction tools will be considered, in particular adaptive wavelet analysis to enhance the feature extraction from the magnetic signature.

Acknowledgment

The authors would like to acknowledge the financial support of this project by the New Zealand Science for Technological Innovation National Science Challenge. Sincere thanks to Wayne Crump for his technical support.

References

[1] Y. G. Paithankar and S. Bhide, *Fundamentals of power system protection*. PHI Learning Pvt. Ltd., 2010.

[2] Y. V. Makarov, V. I. Reshetov, A. Stroev, and I. Voropai, "Blackout prevention in the united states, europe, and russia," *Proceedings of the IEEE*, vol. 93, no. 11, pp. 1942–1955, 2005.

[3] D. Yu and S. H. Khan, "An adaptive high and low impedance fault detection method," *IEEE Transactions on Power Delivery*, vol. 9, no. 4, pp. 1812–1821, 1994.

[4] C. Fernandez, "An impedance-based ct saturation detection algorithm for busbar differential protection," *IEEE Transactions on power delivery*, vol. 16, no. 4, pp. 468–472, 2001.

[5] D. J. Richardson and M. C. Thompson, "An analysis of test data selection criteria using the relay model of fault detection," *IEEE Transactions on Software Engineering*, vol. 19, no. 6, pp. 533–553, 1993.

[6] A. Emanuel, D. Cyganski, J. Orr, S. Shiller, and E. Gulachenski, "High impedance fault arcing on sandy soil in 15 kv distribution feeders: contributions to the evaluation of the low frequency spectrum," *IEEE Transactions on Power Delivery*, vol. 5, no. 2, pp. 676–686, 1990.

[7] M. Carpenter, R. Hoad, T. D. Bruton, R. Das, S. A. Kunsman, and J. Peterson, "Staged-fault testing for high impedance fault data collection," in *Protective Relay Engineers, 2005 58th Annual Conference for*. IEEE, 2005, pp. 9–17.

[8] A. Ghaderi, H. L. Ginn, and H. A. Mohammadpour, "High impedance fault detection: A review," *Electric Power Systems Research*, vol. 143, pp. 376–388, 2017.

[9] D. Hou, "High-impedance fault detectionfield tests and dependability analysis," in *proceedings of the 36th Annual Western Protective Relay Conference, Spokane, WA*, 2009.

[10] A. dos Santos and M. C. de Barros, "Stochastic modeling of power system faults," *Electric Power Systems Research*, vol. 126, pp. 29–37, 2015.

[11] S. Gautam and S. M. Brahma, "Detection of high impedance fault in power distribution systems using mathematical morphology," *IEEE Transactions on Power Systems*, vol. 28, no. 2, pp. 1226–1234, 2013.

[12] A. Sedighi, "A new model for high impedance fault in electrical distribution systems," *International Journal of Scientific Research in Computer Science and Engineering*, vol. 2, no. 4, pp. 6–12, 2014.

[13] N. I. Elkalashy, M. Lehtonen, H. A. Darwish, M. A. Izzularab, and I. T. Abdel-maksoud, "Modeling and experimental verification of high impedance arcing fault in medium voltage networks," *IEEE Transactions on Dielectrics and Electrical Insulation*, vol. 14, no. 2, 2007.

[14] A.-E. R. Book, "Canadian," *American EMTP User Group*, vol. 92, 1987.

[15] T. NengLing and C. JiaJia, "Wavelet-based approach for high impedance fault detection of high voltage transmission line," *International Transactions on Electrical Energy Systems*, vol. 18, no. 1, pp. 79–92, 2008.

[16] A. Ghaderi, H. A. Mohammadpour, H. L. Ginn, and Y.-J. Shin, "High-impedance fault detection in the distribution network using the time-frequency-based algorithm," *IEEE Transactions on Power Delivery*, vol. 30, no. 3, pp. 1260–1268, 2015.

[17] A.-R. Sedighi, M.-R. Haghifam, O. Malik, and M.-H. Ghassemian, "High impedance fault detection based on wavelet transform and statistical pattern recognition," *IEEE Transactions on Power Delivery*, vol. 20, no. 4, pp. 2414–2421, 2005.

[18] S. Ziegler, R. C. Woodward, H. H.-C. Iu, and L. J. Borle, "Current sensing techniques: A review," *IEEE Sensors Journal*, vol. 9, no. 4, pp. 354–376, 2009.

[19] Q. Huang, S. Jing, J. Yi, and W. Zhen, "New types of sensors for smart grid," *Innovative Testing and Measurement Solutions for Smart Grid*, pp. 11–80.

[20] Y. Ouyang, J. He, J. Hu, and S. X. Wang, "A current sensor based on the giant magnetoresistance effect: Design and potential smart grid applications," *Sensors*, vol. 12, no. 11, pp. 15 520–15 541, 2012.

[21] Q. Huang, W. Zhen, and P. Pong, "A novel approach for fault location of overhead transmission line with noncontact magnetic-field measurement," in *Power and Energy Society General Meeting (PES), 2013 IEEE*. IEEE, 2013, pp. 1–1.

[22] Q. Huang, W. Zhen, and P. W. Pong, "A novel approach for fault location of overhead transmission line with noncontact magnetic-field measurement," *IEEE Transactions on Power Delivery*, vol. 27, no. 3, pp. 1186–1195, 2012.

[23] S. Mallat and W. L. Hwang, "Singularity detection and processing with wavelets," *IEEE transactions on information theory*, vol. 38, no. 2, pp. 617–643, 1992.

[24] J. Arrillaga and N. R. Watson, *Power system harmonics*. John Wiley & Sons, 2004.

[25] S. N. Ananthan, R. Padmanabhan, R. Meyur, B. Mallikarjuna, M. J. B. Reddy, and D. K. Mohanta, "Real-time fault analysis of transmission lines using wavelet multi-resolution analysis based frequency-domain approach," *IET Science, Measurement & Technology*, vol. 10, no. 7, pp. 693–703, 2016.

[26] MATLAB, "Dwt function," 2017. [Online]. Available: https://au.mathworks.com/help/wavelet/ref/dwt.html/

[27] I. Daubechies, "Orthonormal bases of compactly supported wavelets," *Communications on pure and applied mathematics*, vol. 41, no. 7, pp. 909–996, 1988.

[28] D. PowerFactory, "Version 2017," *DIgSILENT International, Germany*, 2017.

[29] P. Anderson, "Fouad, power system control and stability, vol. 1," 1977.

[30] W. H. Kersting, *Distribution system modeling and analysis*. CRC press, 2012.

[31] C. L. Benner and B. D. Russell, "Practical high-impedance fault detection on distribution feeders," *IEEE Transactions on Industry Applications*, vol. 33, no. 3, pp. 635–640, 1997.

[32] D. Hou, "Detection of high-impedance faults in power distribution systems," in *Power Systems Conference: Advanced Metering, Protection, Control, Communication, and Distributed Resources, 2007. PSC 2007*. IEEE, 2007, pp. 85–95.

[33] A. Berizzi, S. Massucco, A. Silvestri, and D. Zaninelli, "Short-circuit current calculation: a comparison between methods of iec and ansi standards using dynamic simulation as reference," *IEEE transactions on industry applications*, vol. 30, no. 4, pp. 1099–1106, 1994.

[34] D. Sweeting, "Applying iec 60909, short-circuit current calculations," in *Petroleum and Chemical Industry Conference (PCIC), 2011 Record of Conference Papers Industry Applications Society 58th Annual IEEE*. IEEE, 2011, pp. 1–6.